Numerical computation and experimental verification of the emitted sound power of a vibrating baffled piston into a hemi-anechoic room

M. Schmelzer, V. Wittstock, C. Bethke
Physikalisch-Technische Bundesanstalt (PTB), Bundesallee 100, 38116 Braunschweig, Germany, Email: martin.schmelzer@ptb.de

Introduction

In many situations, the amount of emitted sound power must be known, e.g. several European directives require machinery to be labelled accordingly [1]. Of course, the values of the sound power should be comparable.

In fact, several methods currently exist to determine the sound power, e.g. [2, 3, 4]. These methods rely on the measurement of the sound pressure and post-calculation of the sound power under special and disputable assumptions concerning the sound field, e.g. ideal free field or ideal diffuse field. The resulting sound powers therefore differ from each other.

If it was possible to construct a sound source whose emitted sound power could be determined using traceable, non-acoustic measurands, this sound source could serve as a realisation of the unit Watt, which could then be disseminated by a substitution method.

One approach to construct such a sound source is a vibrating piston. It gets ascribed the sound power it would emit into an exact free field, e.g. calculated by Rayleigh's integral.

For some special cases, e.g. a rigid piston in an ideal free field, analytical solutions exist. In all other cases, numerical computations are needed.

This paper presents a finite-volume-code for a rotation-symmetrical system in the low-frequency range. The computation results are compared to according analytical results and measurements in a hemi-anechoic room.

Experimental Setup

The piston is installed inside a hemi-anechoic room with a resulting geometry as simple as possible. For construction purposes, the piston was crafted as a circular disk. It is excited by an electrodynamic shaker below. To avoid additional surfaces and edges, this piston-shaker-device was lowered into a cavity. The piston forms an even surface with the floor. The gap was sealed by an O-ring. The field quantities sound pressure and sound intensity are measured on different enveloping surfaces. Figure 1 shows the setup schematically.

Finite Volumes

For the numerical computations, several prerequisites can be listed: First, the piston is a circular disk. For the initial treatment, the system should inherit this rotation symmetry altogether. This routes to cylindrical coordinates. Second, velocities must be prescribed at some boundaries, especially at the piston. The algorithm must either use field quantities or be able to deduce them from energy / power quantities. Third, at other boundaries, impedance- or similar conditions must be prescribed. Fourth, the research aims at validating the emitted sound power. So this quantity must be modelled as exactly as possible. Algorithms with inherent errors in this respect must be avoided.

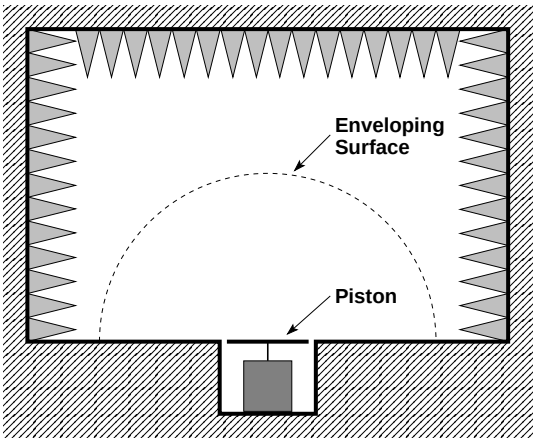

Figure 1: Scheme of hemi-anechoic room and sound source set-up; the piston is driven by a shaker; microphones will be located on enveloping surfaces like the depicted one

For this initial treatment, a finite-volume algorithm was chosen, e.g. [5]. This fulfils conservation of the quantities. As the quantity itself, the potential Φ of the velocity $\underline{v} = -\nabla\Phi$ was chosen, enabling boundary conditions to the velocity. The system will be modelled in the cylindrical coordinates, using radius r and height z. Impedance boundary conditions can be established with respect to the normal component of the velocity field.

The Method

For a given partial differential equation

$$\ddot{\Phi} + \alpha\,\dot{\Phi} = c^2\,\Delta\,\Phi \tag{1}$$

with damping coefficient α and speed of sound c use a harmonic complex ansatz $\Phi(r,z,t) = e^{i\,\Omega\,t}\,\hat{\Phi}(r,z)$ with $i = \sqrt{-1}$, angular frequency Ω and amplitude $\hat{\Phi}$. The damping coefficient α can be deduced from attenuation coefficients given in [6]. Then integrate over the entire volume V of the system and split this integral into disjunct volumes V_j with $V = \bigcup_j V_j$. Then the overall

integral holds if for all j:

$$\int_{V_j} \left(-\Omega^2 + i\,\alpha\,\Omega\right) \hat{\Phi}\; \mathrm{d}V = c^2 \int_{V_j} \operatorname{div} \operatorname{grad} \hat{\Phi}\; \mathrm{d}V \qquad (2)$$

At the right-hand side apply the Gauss theorem, at the left-hand side the mean value theorem:

$$\left(-\Omega^2 + i\,\alpha\,\Omega\right) \overline{\Phi}_j\; V_j = c^2 \oint_{\partial V_j} \left(\operatorname{grad} \hat{\Phi}\right) \cdot \underline{n}\; \mathrm{d}S \qquad (3)$$

with mean values $\overline{\Phi}_j$. This equation is sufficient for the interior of the region, if $\operatorname{grad} \hat{\Phi}$ is expressed by the mean values $\overline{\Phi}_j$. This can be done by a difference scheme. At the boundaries, $\underline{\hat{v}} = -\operatorname{grad} \hat{\Phi}$ immediately enables velocity conditions and even impedance conditions for the normal component of $\underline{\hat{v}}$:

$$\underline{\hat{v}} \cdot \underline{n} = \frac{1}{Z}\,\hat{p} = \frac{1}{Z}\,\rho\, i\,\Omega \hat{\Phi} \qquad (4)$$

with given impedance Z, amplitude of pressure $\hat{p}$, mass density ρ and unit normal vector of the boundary $\underline{n}$.

This finally yields an inhomogeneous, banded system of linear equations for the vector of the mean values $\overline{\Phi}_j$ which is then solved using an adapted Gauss algorithm. First, a uniform mesh of cuboid-shaped volumes was used. Later, the mesh was locally refined in several steps in the vicinity of the piston.

The region covers the ranges: $0\,\mathrm{m} \le r \le 4\,\mathrm{m}$ for the radius and $0\,\mathrm{m} \le z \le 6\,\mathrm{m}$ for the height. The piston is located at $z = 0\,\mathrm{m}$ and $r \le 0.049\,\mathrm{m}$. In this area, the velocity of the piston is prescribed as velocity boundary condition for the normal component of the velocity field. For all other positions at $z = 0\,\mathrm{m}$ and for all $r = 0\,\mathrm{m}$, the normal component of the velocity field is zero. The former because a rigid floor is assumed, the latter because of the symmetry condition. At $r = 4\,\mathrm{m}$ and at $z = 6\,\mathrm{m}$, a free-field impedance boundary condition with $Z = \rho\, c$ is implemented according to eqn. (4).

Comparison with analytical solutions

For a validation of the numerical algorithm, its results will be compared to some existing analytical solutions.

First, for a rigid circular piston, the sound pressure can be calculated along the z-axis, i.e. for $r = 0\,\mathrm{m}$. The exact solution is (e.g. in [7]):

$$p(z) = \rho\, c\, v_0\, e^{-2\pi i\, z/\lambda} \left[1 - e^{-2\pi i\,(\sqrt{r^2+z^2}-z)/\lambda}\right] \qquad (5)$$

with the velocity amplitude v_0 of the piston, the radius r of the piston and the wavelength λ. A comparison for $f = 100\,\mathrm{Hz}$ is shown in figure 2. The numerical result shows some deficiencies starting 1 m above the piston. At about 5 m, the numerical result deviates severely (approx. 10 dB) from the expected course. The reason for both is seen in the incomplete impedance boundary conditions that only involve the normal component of $\underline{v}$.

Second, the numerically calculated emitted sound power of the piston is compared to the emitted sound power of some elementary emitters: a point source, a sphere and a piston, whose sound powers are given by (e.g. from [8]):

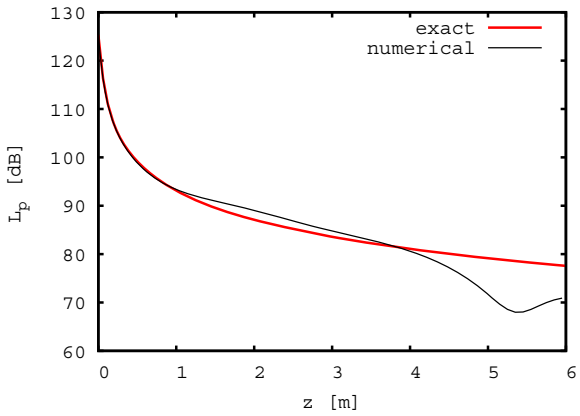

Figure 2: Comparison of the sound pressure level L_p along the z-axis for $f = 100\,\mathrm{Hz}$; exact solution from eqn. (5)

$$\begin{aligned} P_{point} &= \rho c \quad \tilde{Q}^2 \tfrac{2}{4\pi} \quad k^2 \\ P_{sphere} &= \rho c \quad \tilde{Q}^2 \tfrac{2}{4\pi} \quad \tfrac{k^2}{1+(k\overline{r})^2} \\ P_{piston} &= \rho c \quad \tilde{v}^2 \pi\, r^2 \quad \left(1 - \tfrac{J_1(2kr)}{kr}\right) \end{aligned} \qquad (6)$$

with the amplitude $\hat{v}$ of the piston velocity, the effective velocity $\tilde{v} = \hat{v}/\sqrt{2}$, the volume flow $\tilde{Q} = \pi\, r^2\, \tilde{v}$, the radius r of the piston, the equivalent radius of the sphere $\overline{r} = r/\sqrt{2}$, the wave number k and Bessel's function of the first kind and first order J_1. For the numerical result, the emitted sound power of the piston is calculated directly at the piston surface by the formula

$$P = \frac{1}{2} \int_{A_{piston}} \operatorname{Re}\left(p^*\, \underline{\hat{v}}\right) \cdot \underline{n}\; \mathrm{d}S \qquad (7)$$

with the complex conjugate of the sound pressure p^*, the amplitude of the velocity vector $\underline{\hat{v}}$ and the surface of the piston A_{piston}. A comparison is shown in figure 3.

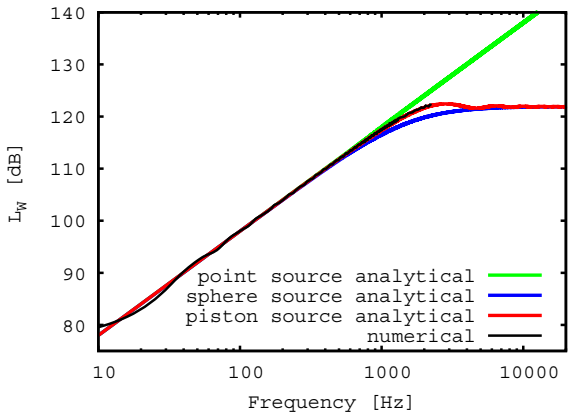

Figure 3: Comparison of the sound power levels L_W of the numerically calculated piston and some elementary emitters calculated from eqn. (6)

As expected, the numerical result follows the values of the elementary piston emitter. Some deviations still exist, staying below 0.5 dB above 50 Hz.

Analysis of numerical results

As shown in figure 3 before, some differences still exist between the numerically and the analytically computed results. In the following figures, the sound power difference referred to the point source will be shown.

It was found that the periodicity of the difference changed severely when the radius of the geometry was varied, but remained nearly unchanged when the height was varied. This is shown in figures 4 and 5.

It is not clear yet, why the system reacts so significantly to changes in radial direction r and nearly not at all to changes in axial direction z – although both directions feature the same set of boundary conditions: isolation at $r = 0$ and at $z = 0$ (except at the piston region) and free field impedance at $r = 4\,\mathrm{m}$ and $z = 6\,\mathrm{m}$.

The amount of the difference can be reduced when the discretisation is refined. This is shown in figure 6.

Above 50 Hz the differences can be gradually reduced using finer meshes. It is expected that the effect continues for even finer discretisations. Below 50 Hz the differences remain nearly constant. This can't be explained yet.

The reason for the existance of the periodical differences is seen in the incomplete impedance boundary conditions using only the normal component of the velocity field: For non-perpendicular incidence the boundary condition results in some amount of reflection. It was attempted to reduce this by randomly adding additional damping within a region of 1 m in front of the outer wall and the ceiling. This is similar to the technical realisation of an anechoic room as suggested by Cremer. But this had no effect.

Comparison with measurements

Measurements were performed in the hemi-anechoic room of PTB. The geometric parameters of the numerical calculation were similar to those of the room. The excitation velocity of the numerical calculation was scaled according to the measured one which was taken by a single accelerometer in the center of the piston.

Sound pressure and sound intensity were taken at ten positions forming an enveloping mesh around the source and the sound power was calculated therefrom. Pink noise was used to excite the system and measurements were filtered using third-octave bands.

Figure 7 shows the results of the measurements and of the corresponding numerical computations. There is a good agreement in the frequency range from 100 Hz to 1000 Hz. Differences below 100 Hz are seen to result from sound emissions from the surrounding baffle which became excited by the built-in piston due to friction. Differences above 1000 Hz are expected to result from the first eigenmodes of the piston. This has to be examined further.

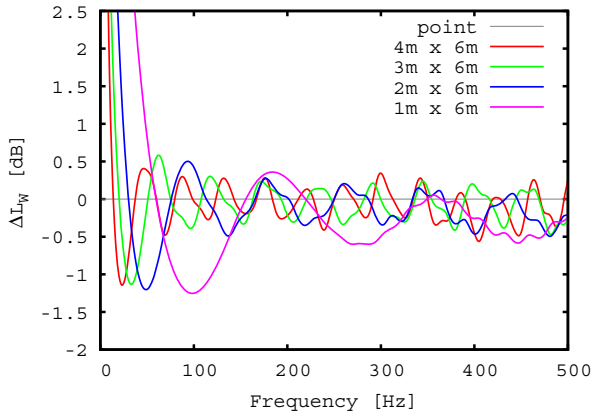

Figure 4: Sound power difference ΔL_W (refered to point source); variation of radius by compressing the parameter r and the volumes of calculation in the same manner; for $r = 4\,\mathrm{m}$ (red curve) the periodicity of 42 Hz belongs to a wavelength of 8 m (double of radius)

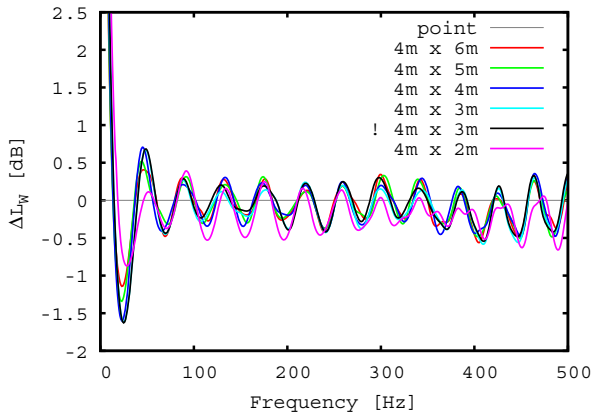

Figure 5: Sound power difference ΔL_W (refered to point source); variation of height, mostly by compressing the parameter z and the volumes of calculation in the same manner, but once also with adjusted discretisation (curve with !)

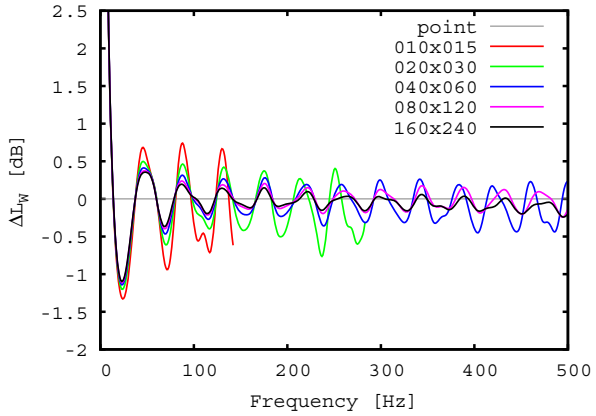

Figure 6: Sound power difference ΔL_W (refered to point source); variation of discretisation (given numbers of volumes)

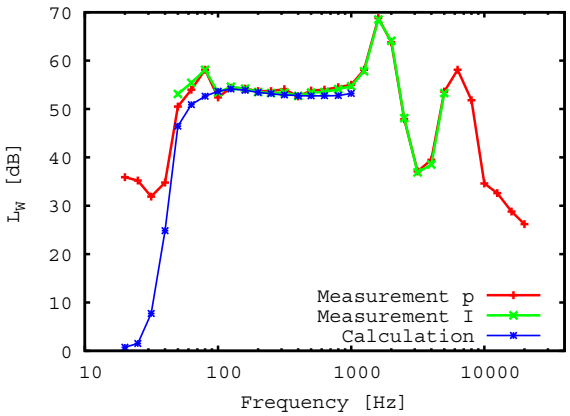

Figure 7: Comparison of the sound power levels L_W of the measurements using pressure and intensity methods and the according numerical computation

Conclusions

Although the field quantity of sound pressure shows some severe deviations from the expected analytical result (approx. 10 dB), the deviations of the integral quantity sound power stay below 0.5 dB above 50 Hz and can also be reduced further by globally refining the discretisation mesh. Within 100 Hz to 1000 Hz, a good agreement with measurements is achieved with respect to third-octave band filtering.

References

[1] EU Directive 2010/30/EU

[2] DIN EN ISO 3745, Acoustics – Determination of sound power levels and sound energy levels of noise sources using sound pressure – Precission methods for anechoic rooms and hemi-anechoic rooms, Beuth, 2012

[3] DIN EN ISO 3744, Acoustics – Determination of sound power levels and sound energy levels of noise sources using sound pressure – Engineering methods for an essentially free field over a reflecting plane, Beuth, 2011

[4] DIN EN ISO 3741, Acoustics – Determination of sound power levels and sound energy levels of noise sources using sound pressure – Precision methods for reverberation test rooms, Beuth, 2011

[5] Charles Hirsch: Numerical computation of internal and external flows. Wiley & Sons, Chichester, 1988

[6] ISO 9613-1, Acoustics – Attenuation of sound during propagation outdoors – Part 1: Calculation of the absorption of sound by the atmosphere, Beuth, 1993

[7] Michael Möser: Technische Akustik. Springer, Berlin, 8th ed., 2009

[8] Eugen Skudrzyk: Die Grundlagen der Akustik. Springer, Wien, 1954